Type of the Paper (Article)

Development and application of a nano-coated selective electrode for detection of iron in wastewater

Aziz Salih Aziz Ajumaily[1], Shatha Y. Al Samarrai[1*]

[1] Chemistry Department, College of Science, Tikrit University, Iraq.
[*]Corresponding Author: dr.shatha81@tu.edu.iq

Abstract: This study investigates the possibility of determining iron in wastewater using the green chemistry method, including developing an iron-selective electrode coated with nano CG-FeO- NPs extracted from mint leaves. The developed electrode was characterised using AFM, SEM, XRD and IR technologies. The performance of the new electrode was optimised for the effects of the pH, temperature and response time. The results showed that the electrode works efficiently in a pH range of 5-8, a temperature range of 20-30 ^{o}C, and a response time of 6-88 seconds. The calibration curve was range line response from 10^{-1} to 10^{-11} with a slope of -28.727 mV/decade, a correlation coefficient of 0.9997, a detection limit of 2.4×10^{-10} M, a lifetime of 48 days and a recovery percentage of 98.5-99,80 for concentrations of $10^{-2}, 10^{-3}$ and 10^{-4}. A selectivity test was also carried out to ensure no interferences with other elements such as zinc, potassium, sulphite, lead, calcium and manganese. Measurements proved that the electrode has high selectivity towards iron ions only and no other elements. Applications were carried out using the standard addition method on an industrial water model and gave a correlation coefficient of 0.9999.

1. Introduction.

Iron is one of the most important metals in biological systems, the environment, industry, and medicine. It is necessary for immunity, growth regulation, oxygen transport, and cell differentiation in human bodies. But too much of this ion might cause toxicity or even fatalities. Consequently, it is crucial to quickly and accurately determine the concentration of Fe(III) in biological and environmental materials. (1,2.3). Since iron is a common element in the rocks that make up the earth's crust, there is a lot of it in groundwater. Dissolved ferrous ions (Fe^{+2}) are the most prevalent type of iron ions found in groundwater., They precipitate at 3 + 10 grams per litre and are insoluble. When they come into contact with the atmosphere, they oxidise, forming ferric ions (Fe^{+3}) and ferric hydroxide, which precipitate and give the water a brown hue. Ferrous ions in the water take the form of binary iron (Fe^{+3}), which transforms into triple iron (Fe^{+2})., which results in numerous issues; therefore, these oxides must be separated before using the water. It is not feasible to use water pipes from the process in oxidation-reduction reactions, which are (Fe – Fe+3 iron), as they will eventually erode. Additionally, this water cannot be used for washing as it will result in brown spots from iron rust. Additionally, since the maximum permitted concentration of ferrous ions in drinking water and domestic use

does not exceed 3.0 mg/litter, the rusting of filter pipes and packaging in groundwater wells is caused by the containment of ferrous ions., since its growth results in rust on utensils and other objects, as well as an unpleasant taste (rust taste) (4).

Iron's impact on health An excessive amount of iron in water is bad for people's health because it can build up in the liver, kill cells, trigger allergies, and even lead to blood disorders like anaemia (5). Human indigestion is caused by excess iron, which combines with drinking water that comes from metal pipes. Hemochromatosis is an iron storage disease that can be problematic for people with drinking water iron concentrations of 2-3 mg/L (6). Birth defects are caused by low concentrations of iron, while poisoning is caused by high concentrations. (7). The field of nanotechnology started to develop in 1958. One part in a billion is what the word "nano" means. Research and development at the atomic, molecular, or macromolecular levels is known as nanotechnology.

The fundamental units of Nano scales are nanoparticles, which are one-dimensional particles with length scales ranging from roughly 1 to 100 nanometres. Because it is possible to produce and process materials in this size range, there has been a recent upsurge in the use of particles in various industries. Due to their wide range of applications and usage in numerous fields, nanomaterials can be used to create a variety of nanomaterials and nanodevices., applications in the fields of biomedicine, electronics, magnetism, optoelectronics, pharmaceuticals, cosmetics, energy, environment, catalysis, and materials. Global investment in nanotechnology research and development has increased due to the technology's potential. The quality of the environment's air, water, and soil could all be greatly enhanced by nanotechnology. (8, 9).

Nanoscale semiconductor metal particles and metal oxides have garnered significant attention lately because of their distinct physical and chemical characteristics in relation to their size. In recent times, a lot of researchers have focused on blending or combining elements to create new compounds. Greater value for advancements in all fields of next-generation technologies, particularly when nanoscale elements are the focus. Lately, different chemical techniques have been used to create nanoparticles in order to create materials with regulated particle morphology. (10) After he discovered the glass electrode at the start of the 20th century (11), which responds to hydrogen ions, these electrodes were developed to become sensitive to ions like Na+, Li+, and K+. Liquid membranes containing cyclic compounds that are electrically neutral were then found to be useful as ionic carriers. Ionic carriers were greatly advanced after 1970 when plasticiser and PVC were combined, as they served as the foundation for the matrix carrier in ionic electrodes. The electrodes are now widely used because these ion-sensitive selective polymeric membranes have been developed and used to estimate many ions of different charges with high efficiency (12).

 Ion-selective electrodes are components of inexpensive, basic analytical instruments, commonly referred to as sensors. (13-16), Environmental pollution has been acknowledged as a problem that nanoscience can solve. (17,18). There have been numerous reported uses of nanotechnology in biomedical and other industries, including cancer therapy, tumour therapy, antioxidants, biosensors, drug delivery, catalytic activities, and antibacterial, anti-inflammatory, and antifungal properties (19, 20). In recent years, scientists and researchers from all over the world have become increasingly interested in producing nanoparticles due to their unique properties, which include surface photoluminescence (SPR), and biological, optical, and electrical qualities (21).

Metal nanoparticles, including those of gold, nickel, silver, platinum, zinc, and copper, have been produced (22–27). Among these nanoparticles, copper nanoparticles (Cu-NPs) stood out for their unique features, which can be linked to their physical attributes like morphology, crystalline structure, and composition. Cu-NPs also showed good heat transfer properties and were less dangerous and more affordable. (28). Cu-NPs also have the remarkable qualities of being easily produced and easily modified into the desired shape and size of nanoparticles (29). Cu-NPs' biological activity made it a useful source for the synthesis of antibiotics (30). The physical and chemical methods that include the use of sensor chemical preparation approach (28), chemical precipitation methods (31), laser ablation methods (32), solid-state reaction procedure (33), irradiation via gamma ray, and sol-gel have all been adopted for the synthesis of Cu-NPs. (34-38).

The research aims to explore the significance of iron in biological systems and its environmental impact, investigate health implications of varying iron concentrations in water, delve into nanotechnology focusing on nanoparticles' diverse applications, evaluate the unique features and synthesis methods of copper nanoparticles (Cu-NPs), assess advancements in nanoscale metal particles, and understand the development and use of ion-selective electrodes for analytical instruments and environmental remediation.

2. Materials and Methods.

2.1. Chemicals.

The 99% ferric chloride (FeCl3) was purchased from BDH Company, and Di-butyl phthalate (C16H22O4 98 %) was purchased from Fluka. Polyvinyl chloride (-CH_2-CHCl-)$_n$ 98% from Fluka, Potassium chloride (KCl) 99% MERCK, Sodium Hydroxide(NaOH) 99 % from BDH, Tetra hydrofurane (C_4H_8O) 99.9% BDH, Hydrochloric Acid HCl 37% Fluka. All of the chemical substances were analytical grade and were used exactly as supplied, requiring no additional purification.

2.2. Mint Leaf Extract Preparation Process: A Detailed Procedure.

After thoroughly washing the mint leaves with distilled water to remove any dust and dirt, they are air-dried. Subsequently, 50 g of dried mint leaves are weighed and immersed in 500 ml of distilled water overnight. The extracted solution is transferred to a 500 ml dark beaker and refrigerated for later use. A mixture of 50 ml of peppermint extract solution and 50 ml of ferric chloride solution is heated at 80°C with stirring for 2 hours. After cooling, the solution is centrifuged at 3000 rpm for 15 minutes, followed by drying the precipitate in an oven at 100°C for a day. The precipitate is then incinerated using a firing furnace at 400°C for three hours. The resulting product is cooled, finely ground, sifted, and stored in a dry test tube (7,8,9).

2.3. Preparation of Tea Leaf Extract.

Weigh 10 grams of tea leaves and place them in a glass beaker. Add 100 ml of deionised water while continuously stirring using a magnetic stirrer. Heat the mixture to boiling at a temperature of 60 degrees Celsius for 30 minutes. Allow it to cool to room temperature. Filter the cooled mixture through a 0.45-micron filter to obtain a clear tea leaf extract. Take 12 ml of the filtered tea leaf extract and gradually add it to 100 ml of 1mM $AgNO_3$ silver nitrate solution under dark conditions and at room temperature.

2.4. PVC Coating of Graphite Electrodes.

Dissolve 0.1900 g of PVC powder in 5 ml of tetrahydrofuran (THF) with continuous mixing until completely dissolved. Next, add 0.1 g of FeO to the mixture and continue mixing. Incorporate 0.35 ml of di-butyl phthalate into the mixture while stirring. Retrieve a graphite electrode from a mercury-free 777 battery and clean it by immersing it in a sulfuric acid solution for a specific duration. The coating process involves immersing the graphite electrode multiple times in a coating solution until a uniform membrane layer forms on the surface of the graphite electrode. Allow the electrode to dry overnight in the laboratory. Subsequently, immerse the dried coated electrode in a 10^{-2} M ferric chloride solution for a specific duration to complete the ion exchange process. See Figure 1.

Figure 1: Preparation of nano substance and electrode construction.

2.5. Multimodal Characterisation of Iron Oxide Nanoparticles: AFM, SEM, FT-IR, and XRD Analysis.

The surface morphology of the newly synthesised material was analysed using an Atomic Force Microscopy (AFM) device manufactured in the United States. AFM is a powerful imaging technique capable of examining a wide range of surfaces, including biological samples, glass, ceramics, polymers, and composites. It enables the measurement and localisation of various surface properties such as surface morphology, average grain size, and surface uniformity.

Scanning Electron Microscopy (SEM) was employed to characterise the iron oxide nanoparticles. The SEM images provided a cross-sectional view of the nanoparticles, revealing their structure and morphology. Additionally, Fourier Transform Infrared Spectroscopy (FT-IR) using Shimadzu Japan equipment was utilised to identify any organic groups present in the formation of iron nanoparticles using mint leaf extract.

Furthermore, X-ray Diffraction (XRD) analysis was conducted to determine the dimensions and structure of the crystalline nanoparticles. The diffraction pattern obtained from XRD provided insights into the translational symmetry, unit cell size, and electron density of the nanoparticles.

Electrochemical measurements, including potential with millivolt (mv) readings, were performed using a standard calomel electrode (ORION, model ME-SC900) from Britain,

connected to a pH meter (WTW7110) from Germany. Various parameters such as pH effect, temperature effect, response time, calibration curve, selectivity, electrode lifetime, and potential applications were evaluated (28).

3. Results and Discussion.

3.1. AFM Microscopy of FeO NPs.

The AFM measurement of Iron nanoparticles shown in Figure 2 shows the two-, three-dimensional and linear searches extracted from the AFM images of the Iron nanoparticles. Through these images, the shape of the surface topography and the total height of the surface recorded by the AFM is 40.51 nm, the average diameter is 135.1 nm, and the roughness of the surface is Ra=5.395 nm, the high average is 7.484 nm and the shape is The semi-spherical and particle size obtained through this device are almost identical with the results and close to the results of the SEM technique (10,11).
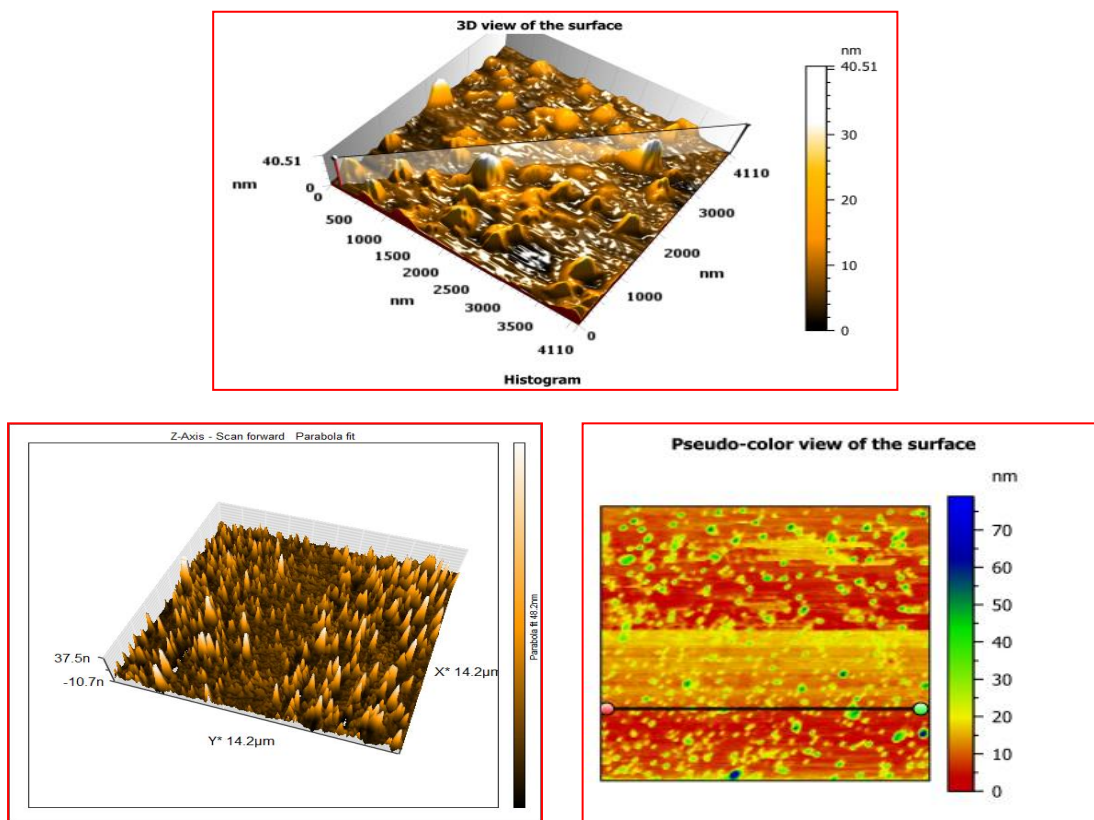

Figure 2: A, B: Surface of Nano Substance (FeO NPs), C: 3D view of the surface of the FeO NPs.

3.2. SEM Microscopy of FeO NPs.

Scanning electron microscopy (SEM) measurements of Iron Oxide nanoparticles The figure below shows a cross-sectional image of the shape and alignment of the Iron Oxide nanoparticles prepared using an SEM at a power of 200 nm; figure 3 shows nanoparticles volume 26.80 nm (35,36).
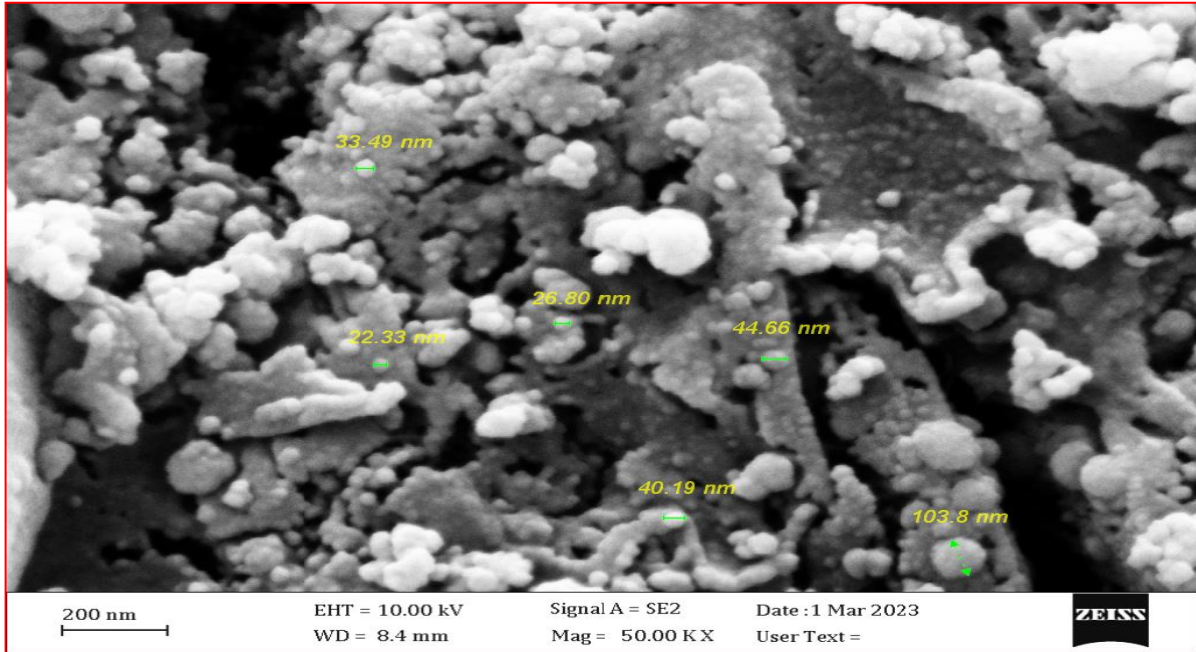
Figure 3: SEM Microscopy of FeO NPs.

3.3. FTIR Spectrum of FeO NPs.

FT-IR revealed the presence of an (O-H) group at a frequency of 3282.8 cm^{-1}, indicating the presence of alcohols in the mint leaves extract such as (polyols, hydroxy flavones, catechins) as shown in Figure 4, (C-C) at a frequency of 1647. 21,1636.34 cm^{-1} indicates the presence of an aromatic component in the mint leaves extract (C-N) at a frequency of 1554.63, 1519.41 cm^{-1}, while groups appeared at 667.37, 640.37 cm^{-1}, showing the presence of (terpenoids), which are the largest class of secondary metabolites of plants (18,23)
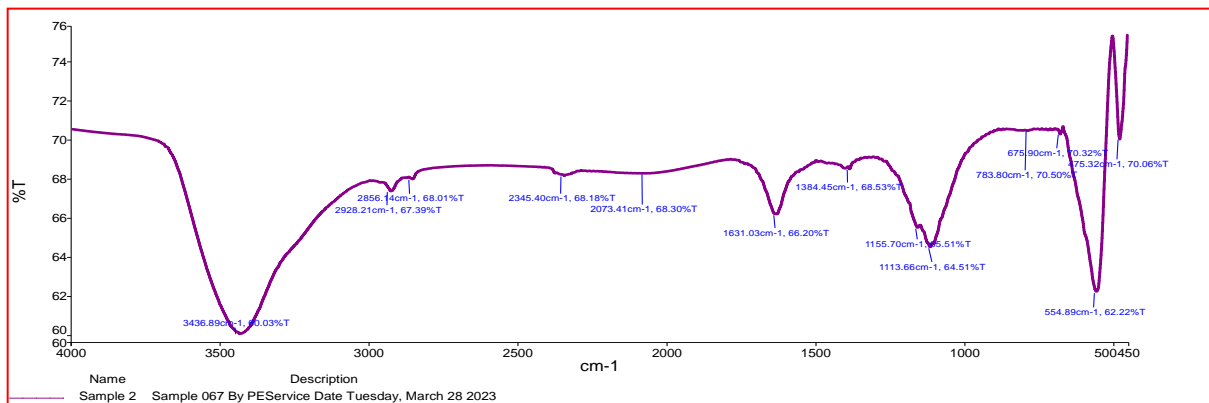

Figure 4: FTIR Spectrum of FeO NPs.

3.4. XRD Spectrum of FeO NPs.

The crystalline nature of the FeNPs was examined using X-ray diffraction. He mentioned that the atoms were crystalline (16,33). The average crystal size of the FeNPs was estimated at 40.165 nm according to the Scherrer equation (44) to calculate the size of the crystals(25), as shown in Figure 5 and Table 1.
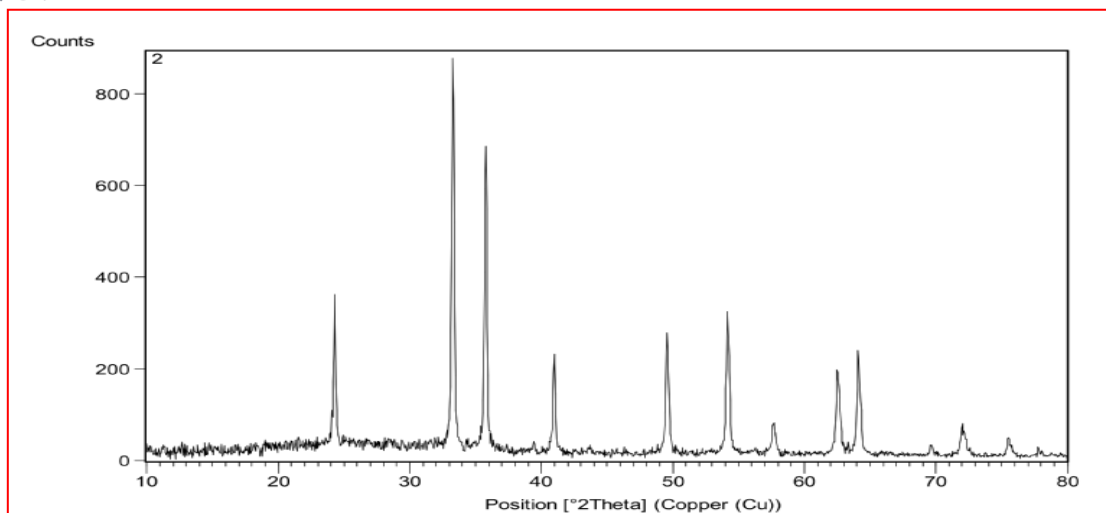
Figure 5: XRD spectrum of prepared Nano Iron Oxide (FeO).

Through the values below, the average size of the prepared nanoparticles of Iron oxide was calculated by applying the Scherrer equation 22,34 in 40.1566 nm.

Table 1: XRD diffraction values and nanoparticle sizes for FeO NPs.

NO.	Pos. [°2Th]	FWHM [°2Th]	D-spacing	Height [cts]	Rel. Int . [%]	Dnm	Average Dnm
1	24.2822	0.1968	3.66554	335.28	38.88	43.14	
2	33.2799	0.1968	2.69223	862.37	100	44.02	
3	35.7589	0.1968	2.51107	668.09	77.47	44.32	
4	40.9974	0.1476	2.20151	215.52	24.99	60.04	
5	49.57	0.1968	1.839	270.55	31.37	46.46	
6	54.1397	0.246	1.69408	324.49	37.63	37.90	40.1566
7	57.6313	0.246	1.59948	64.3	7.46	38.51	
8	62.512	0.3444	1.48582	183.06	21.23	28.20	
9	64.0893	0.1968	1.45301	235.42	27.3	49.77	
10	69.6502	0.2952	1.34998	20.59	2.39	34.26	
11	72.0609	0.3936	1.31064	60.26	6.99	26.08	
12	75.5569	0.36	1.25741	37.91	4.4	29.18	

3.5. Effect of pH.

The best pH range was between 5 and 8. It observed that with the pH decrease, the potential will increase because hydrogen ion release in the solution ,But In the case of an increase in pH, it forms a precipitate when the base is added. The voltage is reduced because of the damaged coated layer on the electrode (24 -31), see figure 6.
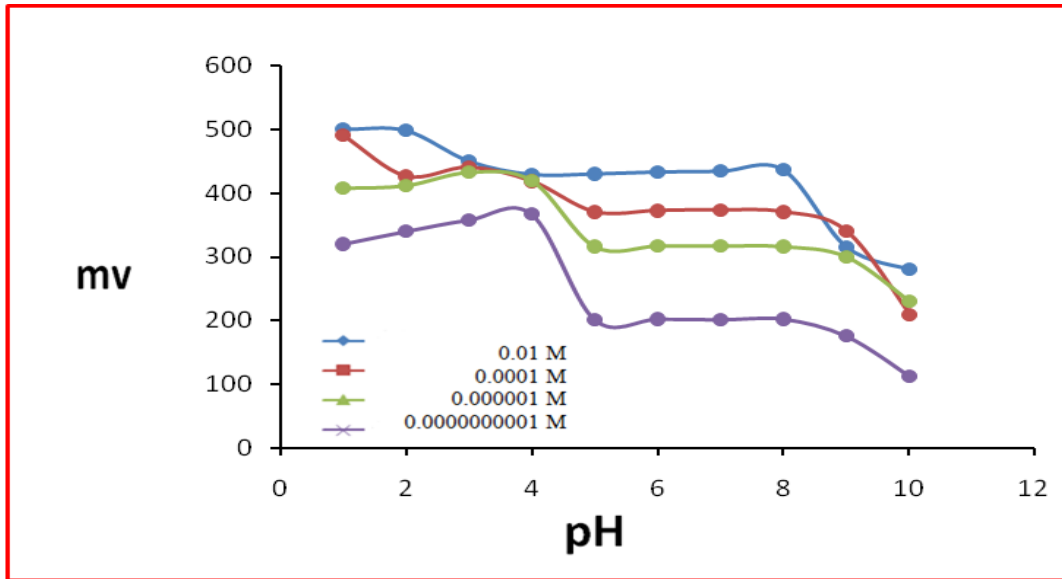
Figure 6: pH Effect on FeO NPs.

3.6. Effect of Temperature.

The effect of temperature was studied in a range of 5-50 °C, as it was noted that the best range of temperature in which the electrode operates without significantly affecting the voltage was between 20 to 30 °C and it turns out that there is a significant rise at higher temperatures in the voltage difference results at 30 °C which may happen as a result of both the manufactured electrode membrane's increased surface area and the increased mobility of Fe^{+2} molecules in the solution outside the electrode. As demonstrated in (27,34) Figure 7, the increase in temperature directly correlates with an increase in the movement of solution ions and the membrane's surface area.
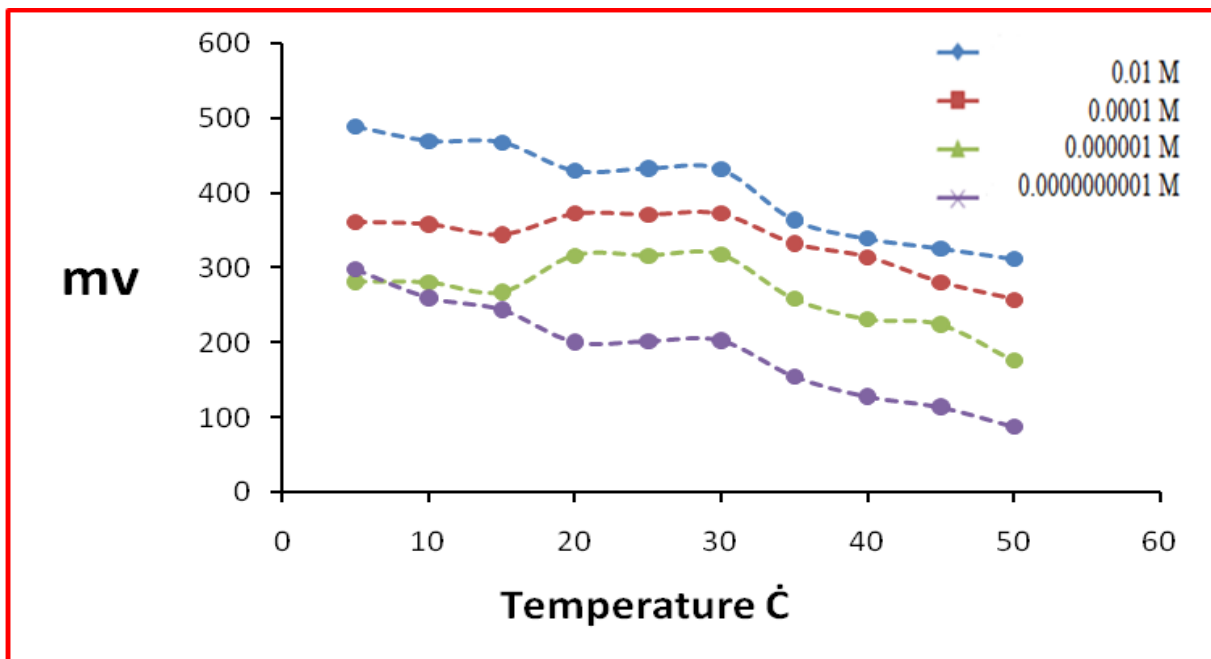

Figure 7: Effect of Temperature on FeO NPs.

3.7. Response Time

The response time for the manufactured probe is depicted in Figure 8. It is noted that the electrode's response time is inversely proportional to the concentration of ions in the external solution and that it ranges within a concentration range of $10^{-1} - 10^{-11}$ molar ranges between 6–88 seconds. Because the ions can more easily reach the electrode's outer membrane when their concentration in the external test solution rises, the response time decreases as well. Conversely, when the concentration of ions falls, fewer ions are present in the external solution, which means it takes longer for the potential electrode to reach an equilibrium state (16,21,35).
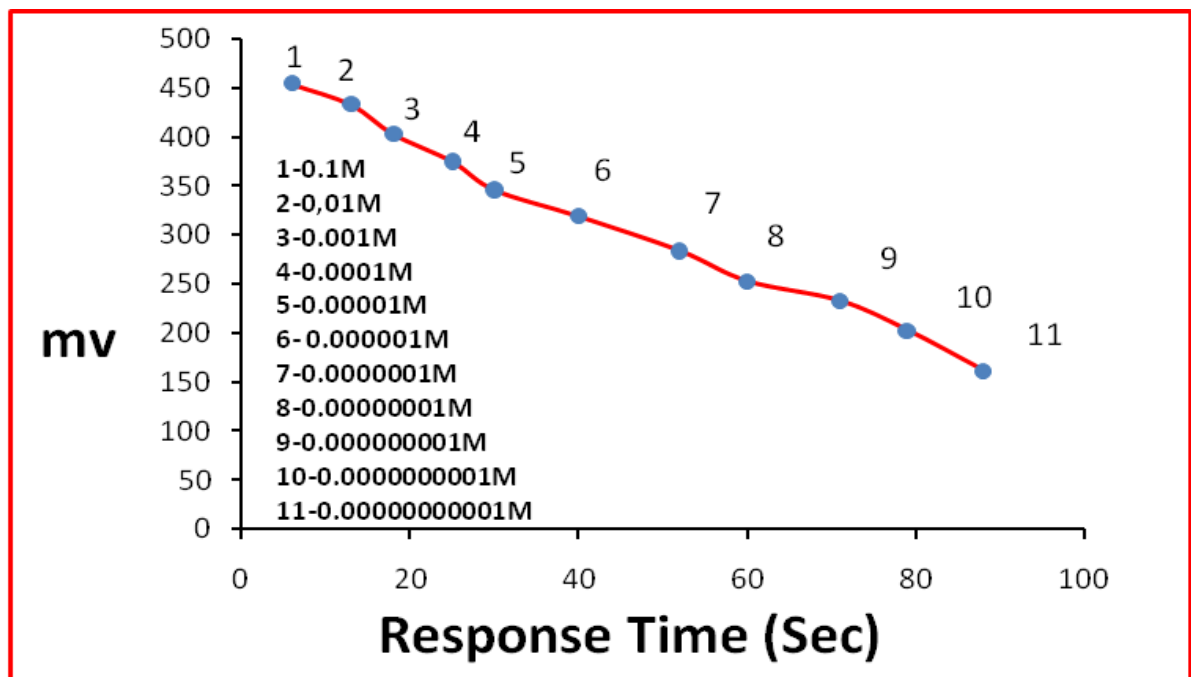

Figure 8: Effect of Response on FeO NPs.

3.8. Calibration Curve

Figure 9 shows the standard electrode curve. The Nernstian response's linear range fell between 10^{-1}-10^{-11} molar, the value of the correlation coefficient was 0.9997, and the slope given by the electrode was -28.727mv/decade, which was close to the true value of the Nernesti slope 29 mv/decade (12, 26).
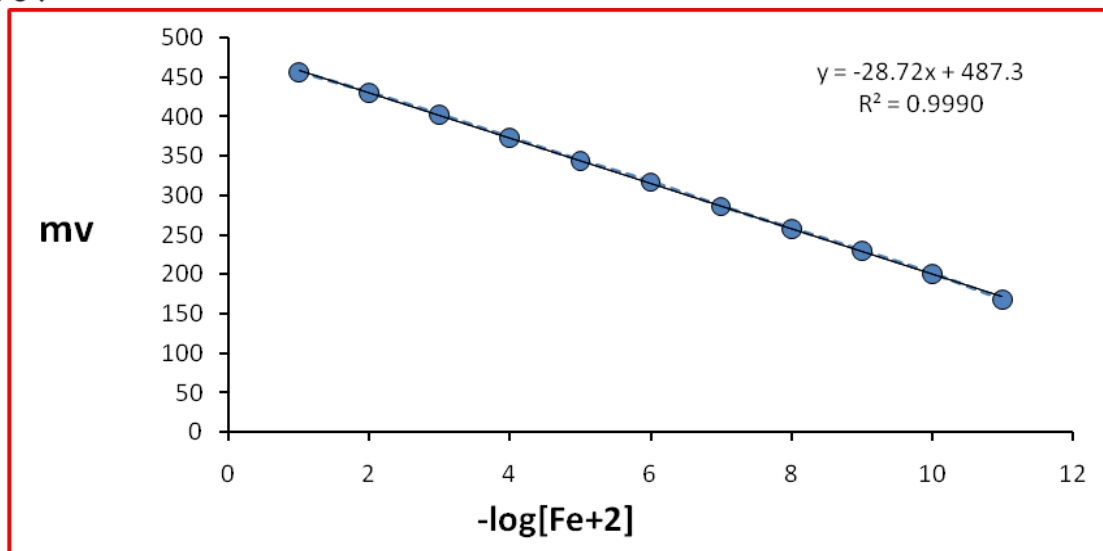
Figure 9: Calibration Curve for FeO NPs Electrode.

3.9. Accuracy and Precision.

After drawing the calibration curve for the electrode, the accuracy and compatibility were studied by measuring the voltages for different concentrations of aqueous Iron Chloride solution located within the linear range of the electrode's response to the calibration curve (2,4), not six readings, and the results are as shown in the following table 2.

Table 2: Accuracy and Precision Value.

Rec %*	RE%*	RSD %*	Measurement Concentration (M)	Taken concentration (M)	Electrode
98.5	-1.5	0.635	0.00985	0.01	
99.80	-0.20	0.422	0.0009980	0.001	CG- FeO NPs
99.7	-0.3	0.1134	0. 000000997	0.000001	

*Average of six readings

3.10. Detection limit.

The detection limit was calculated for the prepared electrode by taking the lowest concentration taken from the calibration curve that the electrode sensed by measuring its potential six consecutive times, and the results are shown in the following Table 3 (22, 37).

Table 3: Detection limit

Detection limit(M)*	Standard Deviation (SD)(	The lowest concentration (molar) the electrode is sensitive to	Electrode
2.4×10^{-10}	0.9620	10^{-10}	CG - FeO NPs

3.11. Selectivity

One of the most crucial factors influencing the type of selective electrode and the range of applications it can be applied to is its selectivity. Using the mixed solution method, the values of the selectivity coefficient were calculated against the interfering ions, as indicated in the table below. The concentration of the interfering ion and the relative error can be used to express the selectivity coefficient, as shown in Table 4 (6,8,13).

Table 4: Selectivity coefficient values.

K Ag, Bpot Selectivity coefficient values		Interfering Ion 10^{-2}M
of Fe^{+2} Concentration		
10^{-4}	10^{-2}	
0.000006987-	0.00605	Zn^{2+}
0.00000950	-0.00000088	K^{1+}
0.00000366-	0.00000743-	SO_4^{2-}
0.0000001532	0.000001892	Pb^{2+}
-0.0000736	0.000000219	Ca^{2+}
0.000001178	0.000036521-	Mn^{2+}

3.12. Life Time of Electrode.

The age of the electrode was estimated by measuring the voltage difference from one day to the next, using a standard solution of copper ions at a concentration of 10^{-3} M. The age of the electrode was 48 days, after which it was noticed that the voltage difference began to decrease(22.34). The reason for the decrease in electrode life is due to leakage and damage to the coating layer 35, as shown in Figure 10.
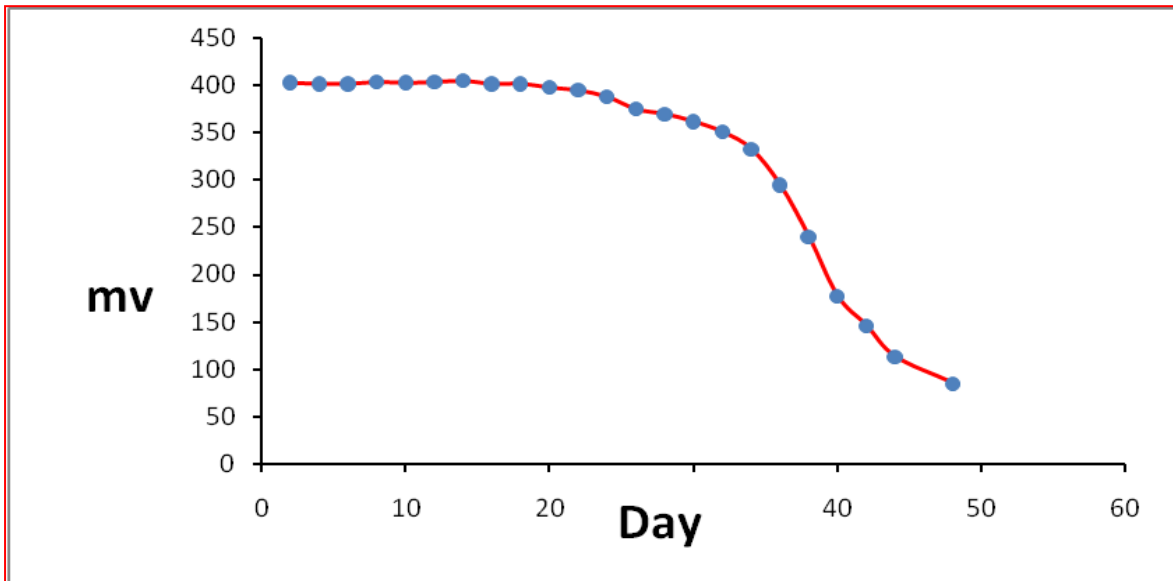
Figure 10: Life Time of Electrode for FeO NPs

3.12.   Applications.

A sample of Iron Chloride was prepared by taking a volume of 2.5 ml of a solution of a concentration of 10^{-3} M in a volumetric Flask of 25 ml and diluting it with tap water. Then 1 ml of the (manufactured sample) was transferred to a series of 6 volumetric flasks of 10 ml capacity, to which increasing volumes 0.5-2 ml of a standard solution of Iron Chloride were added at a concentration of 10 - 2 molar, except for one of the bottles that was left without addition and completed volume with distilled water to the mark. The potential difference was measured for each solution, and the relationship was drawn between Antilog ΔE/S against the volume of the standard solution of added Iron ions; the results are shown in Figure 11 and in Table 5, as the concentration of the studied Iron ions was found in a solution Iron Chloride (22,31,38).
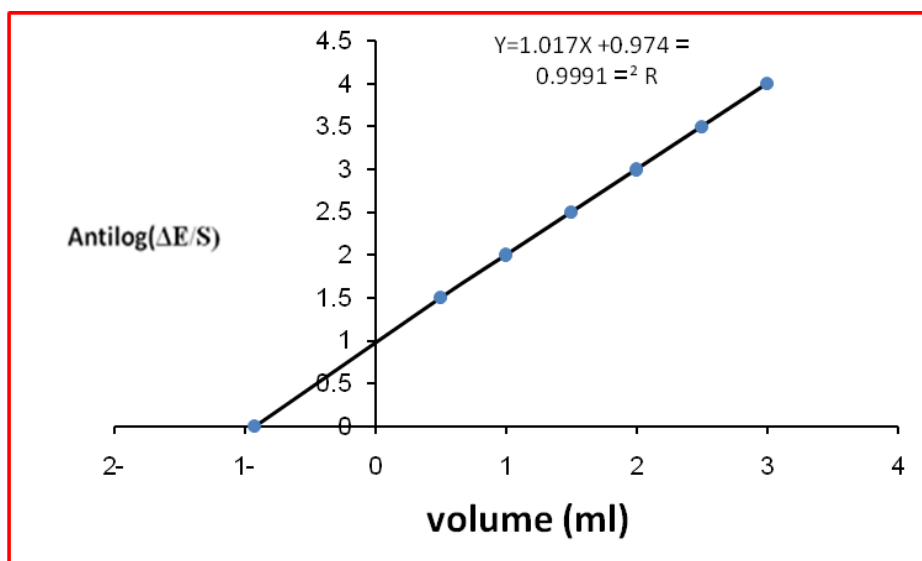

Figure 11: Application curve of the manufactured sample for the determination of copper Fe^{+2} ions

Depending on the straight line equation, and when y = 0, x = 0.93, the volume of the standard solution in ml (Vs) of copper ions at a concentration of 10^{-3} molar, using the following equation :

$$V \quad \ldots\ldots\ldots\ldots(1\text{-}3) \quad\quad\quad\quad\quad\quad / \; C = V_S \, X$$

C: the observed concentration of the solution.

X: The concentration of the studied solution is 10^{-3} M.

V: The volume taken from the standard solution and equal to 1 ml.

VS: the volume of the solution extracted from the equation and equal to 0.93 ml.

Table 5: Applications to the Sample manufactured by the standard addition method

RE %	Rec %	Concentration measured (Molar)	Taken Concentration (Molar)
-3	97	0.00097	10^{-3}

4. Conclusions

An easy, simple, and inexpensive method for the determination of iron in wastewater was developed, relying on natural sources in the preparation of nanoparticles (green chemistry method). This method offers a broad-ranging, fast, sensitive, and wide-ranging approach to determining the concentration of iron ions in aqueous solutions. Moreover, the materials used in the manufacture of the nanomaterial are simple and available, requiring very small quantities. The possibility of applying this method easily to monitor environmental pollution caused by the presence of iron in industrial water discharged by oil refineries is a significant advantage. Furthermore, there is potential for developing the method in the future using new nanomaterials that are available in nature and environmentally friendly, thus contributing to advancements in nanotechnology.

References
1. Sahoo, S. K., Sharma, D., Bera, R. K., Crisponi, G. & Callan, J. F., 2012. Iron(iii) selective molecular and supramolecular fluorescent probes. Chem. Soc. Rev., 41, pp. 7195–7227.
2. Xu, H., Zhou, S., Liu, J. & Wei, Y., 2018. Nanospace-confined preparation of uniform nitrogen-doped graphene quantum dots for highly selective fluorescence dual-function determination of Fe3+ and ascorbic acid. RSC Adv., 8, pp. 5500–5508.
3. Kang, S., Han, H., Lee, K. & Kim, K. M., 2022. Ultrasensitive detection of Fe3+ ions using functionalised graphene quantum dots fabricated by a one-step pulsed laser ablation process. ACS Omega, 7, pp. 2074–2081.
4. Mohammed, N. H. H., 2012. Removal and Re-Use of Iron Oxide Extracted From the Drinking Water in Mahroka District. University of Libya Libyan Agriculture Research Center Journal International, 3(S2), pp. 1416-1428.
5. Hansen, N.C., Hopkins, B.G., Ellsworth, J.W. & Jolley, V.D., 2006. Iron nutrition in plants and rhizospheric microorganisms. In: Sustainable Agriculture Reviews, 41, Springer, pp. 23-59.

6. Weng, H.-X., Qin, Y.-C. & Chen, X.-H., 2007. Elevated iron and manganese concentrations in groundwater derived from the Holocene transgression in the Hang-JiaHu Plain, China. Hydrogeology Journal, 15(4), pp. 715-726.

7. Khan, M.N., Siddiqui, Z. & Uddin, F., 2007. Surfactant-Mediated Catalytic Determination of Fe (II) in Herbal and Pharmaceutical Products. Journal of Surfactants and Detergents, 10(4), pp. 237-242.

8. Hinze, W. L., Pramauro, E., 1993. A critical review of surfactant-mediated phase separations (cloud point extractions)—Theory and applications. Crit. Rev. Anal. Chem., 24 (2), pp. 133–177.

9. Pereira, M. G., Arruda, M. A. Z., 2003. Trends in pre-concentration procedures for metal determination using atomic spectrometry techniques. Microchim. Acta., 141 (3–9), pp. 115–131.

10. Skoog, D. A., Holler, F. J., Nieman, T. A., 1998. Principles of Instrumental Analysis. 4th Ed., Saunders College Publishing, Florida, p. 367.

11. Pungor, E., 2001. The New Theory of Ion-Selective Electrodes. Sensors, (1), pp. 1-12.

12. Kirking, S., Nordquist, E., 2005. Introduction to Ion-Selective Electrodes in the Classroom and their Application to the Real World. Nat. Sci. Foundation Grant, (3), pp. 1-20.

13. Fei, H., Barron, A. R., 2012. Introduction to Ion Selective Electrode. Available at: http://cnx.org/lenses/ricescholarship/affiliation, May 30.

14. Han, Q., Yang, X., Huo, Y., Lu, J., Liu, Y., 2023. Determination of Ultra-Trace Amounts of Copper in Environmental Water Samples by Dispersive Liquid-Liquid Microextraction Combined with Graphite Furnace Atomic Absorption Spectrometry. Separations, 10, 93.

15. Hashem, E. Y., Seleim, M. M., El-Zohry, A. M., 2011. Environmental method for spectrophotometric determination of copper(II). Green Chemistry Letters and Reviews, Vol. 4, No. 3, September.

16. Leel, T., Lia, S., Ray, M., 2007. Greener analytical method for the determination of copper(II) in wastewater by micro flow system with optical sensor. Talanta.

17. Adewale, S., Kolawole, A., Charles, S., Felix, D., 2021. Green chemistry approach towards the synthesis of copper nanoparticles and its potential applications as therapeutic agents and environmental control. ELSEVIER, Volume 4, 100176.

18. Nasrollahzadeh, M., Sajjadi, M., Dadashi, H. J., Ghafuri, P., 2020. Pd-based nanoparticles: plant-assisted biosynthesis, characterisation, mechanism, stability, catalytic and antimicrobial activities. Adv. Colloid Interface Sci., 276, 102103.

19. Meng, F., Sun, H., Huang, Y., Tang, Y., Chen, Q., Miao, P., 2019. Peptide cleavage-based electrochemical biosensor coupling graphene oxide and silver nanoparticles. Anal. Chim. Acta, 1047.

20. Nasrollahzadeh, M., Shafei, N., Nezafat, Z., Soheili Bidgoli, N. S., Soleimani, R. S. F., Varma, R., 2020. Valorisation of fruits, their juices and residues into valuable (nano)materials for applications in chemical catalysis and environment. Chem. Rec., 20, 1–57.

21. Jadoun, S., Arif, R., Jangid, N. K., Meena, R. K., 2021. Green synthesis of nanoparticles using plant extracts: a review. Environ. Chem. Lett., 19, 355–374.

22. Folorunso, A., Akintelu, S., Oyebamiji, A. K., Ajayi, S., Abiola, B., Abdusalam, I., Morakinyo, A., 2019. Biosynthesis, Characterisation and antimicrobial Activity of gold nanoparticles from leaf extracts of Annona muricata. J. Nanostru. Chem., 9 (2), 111–117.

23. Akintelu, S. A., Folorunso, A. S., Ademosun, O. T., 2019. Instrumental characterisation and antibacterial investigation of silver nanoparticles synthesised from Garcinia kola leaf. J. Drug Deliv. Therapeut., 9 (6-s), 58–64.

24. Akintelu, S. A., Folorunso, A. S., 2019. Biosynthesis, characterisation and antifungal investigation of Ag-Cu nanoparticles from bark extracts of Garcinia kola. Stm. Cell, 10 (4), 30–37.

25. Akintelu, S.A., Folorunso, A.S., 2019. Characterisation and antimicrobial investigation of synthesised silver nanoparticles from Annona muricata leaf extracts. J Nanotechnol Nanomed Nanobiotechnol, 6, 1–5.

26. Akintelu, S.A., Folorunso, A.S., Oyebamiji, A.K., Erazua, E.A., 2019. Antibacterial potency of silver nanoparticles synthesised using Boerhaavia diffusa leaf extract as reductive and stabilising agent. Int. J. Pharmaceut. Sci. Res., 10 (12), 374–380.

27. Nasrollahzadeh, M., Mahmoudi-Gom Yek, S., Motahharifar, N., Gorab, M.G., 2019. Recent developments in the plant-mediated green synthesis of Ag-based nanoparticles for environmental and catalytic applications. Chem. Rec., 19, 1–45.

28. Cuevas, R., Dur_an, N., Diez, M.C., Tortella, G.R., Rubilar, O., 2015. Extracellular biosynthesis of copper and copper oxide nanoparticles by Stereum hirsutum, a native white-rot fungus from Chilean forests. J. Nanomater., 16 (1), 57.

29. Balasooriya, E.R., Jayasinghe, C.D., Jayawardena, U.A., Ruwanthika, R.W.D., Silva, R.M., Udagama, P.V., 2017. Honey mediated green synthesis of nanoparticles: new era of safe nanotechnology. J. Nanomater., 1-10.

30. Chung, I.M., Rahuman, A.A., Marimuthu, S., Vishnu, K., Anbarasan, K., Padmini, P., Rajakumar, G., 2017. Green synthesis of copper nanoparticles using Eclipta prostrate leaves extract and their antioxidant and cytotoxic activities. Exp. Ther. Med., 14, 18–24.

31. Akintelu, S.A., Olugbeko, S.C., Folorunso, A.S., 2020. A review on synthesis, optimisation, characterisation and antibacterial application of gold nanoparticles synthesised from plants. Int. Nano Lett., 10, 237–248.

32. Akintelu, S.A., Yao, B., Folorunso, A.S., 2020. A review on synthesis, optimisation, mechanism, characterisation, and antibacterial application of silver nanoparticles synthesised from plants. J. Chem., 12, 1–12.

33. Akintelu, A., Folorunso, A.S., Folorunso, F.A., Oyebamiji, A.K., 2020. Green synthesis of copper oxide nanoparticles for biomedical application and environmental remediation. Hel, 6, 1–12. [Online]. Available: https://doi.org/10.1016/j.heliyon.2020,e04508.

34. Akintelu, S.A., Folorunso, A.S., A Review on Green Synthesis of Zinc Oxide Nanoparticles Using Plant Extracts and its Biomedical Applications, BioNanoSci, 2020. [Online]. Available: https://doi.org/10.1007/s12668-020-00774-6.

35. Akintelu, S.A., Olugbeko, S.C., Folorunso, A.S., Folorunso, F.A., Oyebamiji, A.K., 2021. Potentials of phytosynthesized silver nanoparticles in biomedical fields: a review. Int. Nano Lett., 11, 273–293. [Online]. Available: https://doi.org/10.1007/s40089-021-00341-

36. Palza, H., Delgado, K., Curotto, N., 2015. Synthesis of copper nanostructures on silica-based particles for antimicrobial organic coatings. Appl. Surf. Sci., 357, 86–90. [Online]. Available: https://doi.org/10.1016/j.apsusc.2015.08.260.

37. Caraggs, A., Moody, G.T., Thomas, J.D.R., 1979. PVC Matrix Membrane Ion-Selective Electrodes Construction and Laboratory Experiments. J. Chem. Edu., 51 (8), 541.

38. Evans, A., 1987. Potentiometry and Ion Selective Electrode. John Wiley & Sons, Inc. New York, 150.